Microstructure data accompanying the manuscript: **Homogenization of linear elastic properties of short fiber reinforced composites – A comparison of mean field and voxel-based methods**

Viktor Müller[a], Matthias Kabel[b], Heiko Andrä[b], Thomas Böhlke[a,*]

[a]*Chair for Continuum Mechanics, Institute of Engineering Mechanics, Karlsruhe Institute of Technology (KIT)*
[b]*Fraunhofer ITWM, Flow and Material Simulation*

Abstract

The main contribution of this work lies in the detailed comparison of the predictions of linear elastic properties of mean field homogenization approaches and full field, voxel-based homogenization methods for short-fiber reinforced materials. In the former case, the self-consistent, the interaction direct derivative and a two-step-bounding approach, applying the Hashin-Shtrikman bounds, are used. In the latter case, the boundary value problem for representative volume elements is solved using fast Fourier transformation. Model microstructures with unidirectional aligned and two misaligned fiber configurations are considered exemplarily. Fiber volume fractions of 13%, 17% and 21% and phase contrasts of 44, 100 and 1000 in the elastic moduli have been taken into account. The different homogenization schemes are compared by means of effective directional dependent Young's modulus. This detailed comparison shows that mean field and full field solutions deliver similar results for moderate phase contrasts and volume fractions. Especially in the range of realistic phase contrasts like 44 for a composite of polypropylene and glass, the mean field approaches pose reliable alternatives for full field solution. Large phase contrasts result in relative deviations of up to 68%.

1. General information

Three different microstructures have been considered in the paper. Firstly, a microstructure with unidirectional aligned fibers has been considered. Results affiliated

*Corresponding author
Email addresses:
Viktor Müller: `viktor.mueller@kit.edu`
Matthias Kabel: `matthias.kabel@itwm.fraunhofer.de`
Heiko Andrä: `heiko.andrae@itwm.fraunhofer.de`
Thomas Böhlke: `thomas.boehlke@kit.edu`

with this microstructure are referred to with UD in the following. Secondly, inspired by the orientation distribution of the fiber axes in injection-molded thin plates, two different microstructures with misaligned fiber axes have been considered. Results based on this microstructures are denoted with TP1 and TP2 (thin plate) in the following. All microstructures are generated under a periodicity constraint. In Table 1, the components of the orientation tensors, which have been used to generate the model microstructures, are given. The artificial microstructures have been generated by using GeoDict (www.geodict.de).

Table 1: Components of orientation tensors, used for the generation of the model microstructures

	N_{11}	N_{22}	N_{33}	N_{23}	N_{13}	N_{12}
$\boldsymbol{N}_0^{\text{TP1}}$	0.61	0.36	0.03	0.0	0.0	0.0
$\boldsymbol{N}_0^{\text{TP2}}$	0.80	0.18	0.02	0.0	0.0	0.0
$\boldsymbol{N}_0^{\text{UD}}$	1.0	0.0	0.0	0.0	0.0	0.0

For all microstructures, the fibers have been modeled by cylinders with a length of $l = 200\,\mu\text{m}$ and a diameter of $d = 10\,\mu\text{m}$. Ten different RVEs have been realized for each microstructure type. For all realizations, the fiber volume fraction is assumed to be equal to $c_{\text{F}} = 13\%$. Additionally, for UD, fiber volume fractions of 17% and 21% have been taken into account. In Figure 1, examples for UD and TP1 microstructures are given.

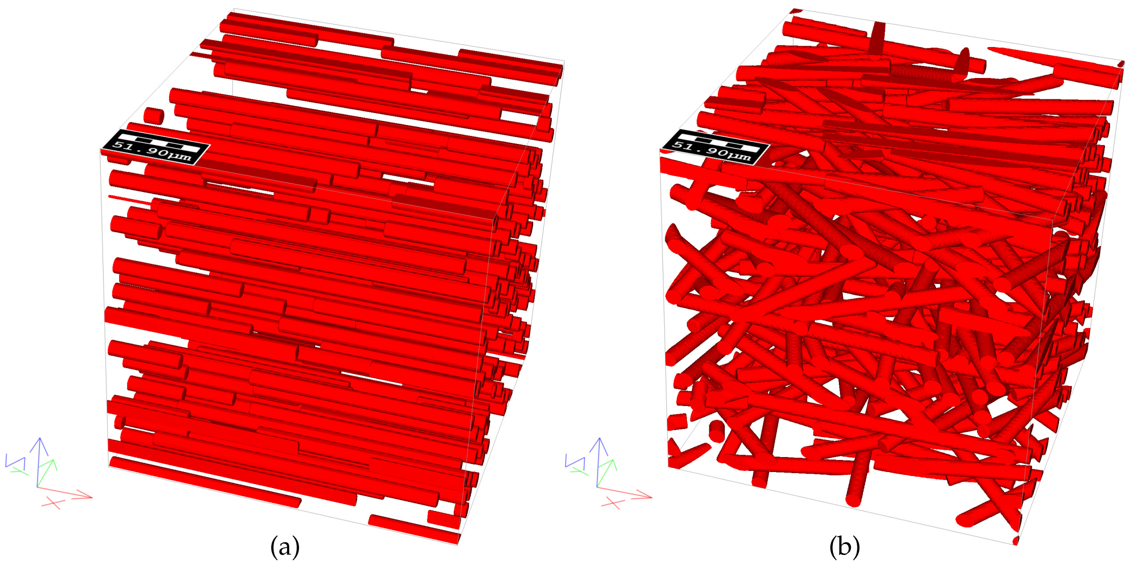

(a) (b)

Figure 1: (a) UD microstructure; (b) TP microstructure.

Each line of the data files contains the direction vector $\boldsymbol{n}$, the position vector to the starting point of the fiber $\boldsymbol{p}$, the length of the fiber l and the diameter of the fiber d. Example for one line in the data is given in Table 2.

Table 2: Example data line

n_x	n_y	n_z	p_x	p_y	p_z	l	d
0.9808	−0.0381	0.1912	8.2312	177.7	143.5	200.0	10.00

All microstructures have been generated periodically. Thus, each line in the data represents a set of fibers, which exhibit a distance of multiple RVE side-lengths in the three spatial directions from each other.

2. Microstructure Data

TP1-configuration with constant volume fraction of 13%:

- **TP1_ZYL_13**
  10 datasets, each with 130 cylindrical inclusion
  RVE side length: $l_{\mathsf{RVE}} = 250\,\mu\mathrm{m}$
- **TP1_ELL_13**
  10 datasets, each with 130 ellipsoidal inclusion
  RVE side length: $l_{\mathsf{RVE}} = 250\,\mu\mathrm{m}$
- **TP1_ZYL_13_rve_size** Variation of the size of the RVE:
  - **small**:
    10 datasets, each with 130 cylindrical inclusion
    RVE side length: $l_{\mathsf{RVE}} = 250\,\mu\mathrm{m}$
  - **medium**:
    10 datasets, each with 1035 cylindrical inclusion
    RVE side length: $l_{\mathsf{RVE}} = 500\,\mu\mathrm{m}$
  - **large**:
    10 datasets, each with 8277 or 8276 cylindrical inclusion
    RVE side length: $l_{\mathsf{RVE}} = 1000\,\mu\mathrm{m}$
- **TP1_ZYL_13_nonPeriodic**
  Microstructures generated **without periodicity constraint** and with variation of the RVE size:
  - **small**:
    10 datasets, each with 618 to 728 cylindrical inclusions
    RVE side length: $l_{\mathsf{RVE}} = 250\,\mu\mathrm{m}$

- **medium**:
  10 datasets, each with 3983 to 4347 cylindrical inclusions
  RVE side length: $l_{\mathsf{RVE}} = 500\,\mu\mathrm{m}$
- **large**:
  10 datasets, each with 23578 to 24037 cylindrical inclusions
  RVE side length: $l_{\mathsf{RVE}} = 1000\,\mu\mathrm{m}$

TP2-configuration with constant volume fraction of 13%:

- **TP2_ZYL_13**
  10 datasets, each with 130 cylindrical inclusion
  RVE side length: $l_{\mathsf{RVE}} = 250\,\mu\mathrm{m}$

UD-configuration:

- **ud_zyl_13**
  10 datasets, each with 130 cylindrical inclusion and a volume fraction of 13%
  RVE side length: $l_{\mathsf{RVE}} = 250\,\mu\mathrm{m}$
- **ud_zyl_13**
  10 datasets, each with 170 cylindrical inclusion and a volume fraction of 17%
  RVE side length: $l_{\mathsf{RVE}} = 250\,\mu\mathrm{m}$
- **ud_zyl_13**
  10 datasets, each with 209 cylindrical inclusion and a volume fraction of 21%
  RVE side length: $l_{\mathsf{RVE}} = 250\,\mu\mathrm{m}$
- **ud_ell_13**
  10 datasets, each with 130 ellipsoidal inclusion
  RVE side length: $l_{\mathsf{RVE}} = 250\,\mu\mathrm{m}$